Inorganic Chemistry

ARTICLE

pubs.acs.org/IC

Coordination of 1,10-Phenanthroline and 2,2′-Bipyridine to Li^+ in Different Ionic Liquids. How Innocent Are Ionic Liquids?

Matthias Schmeisser,[†] Frank W. Heinemann,[†] Peter Illner,[†] Ralph Puchta,[†,‡] Achim Zahl,[†] and Rudi van Eldik*[,†]

[†]Inorganic Chemistry, Department of Chemistry and Pharmacy, University of Erlangen-Nürnberg, Egerlandstrasse 1, 91058 Erlangen, Germany

[‡]Computer Chemistry Center, Department of Chemistry and Pharmacy, University of Erlangen-Nürnberg, Nägelsbachstrasse 25, 91052 Erlangen, Germany

Supporting Information

ABSTRACT: On the basis of ^{7}Li NMR measurements, we have made detailed studies on the influence of the ionic liquids [emim][NTf_2], [emim][ClO_4], and [emim][$EtSO_4$] on the complexation of Li^+ by the bidentate N-donor ligands 2,2′-bipyridine (bipy) and 1,10-phenanthroline (phen). For each of the employed ionic liquids the NMR data implicate the formation of $[Li(bipy)_2]^+$ and $[Li(phen)_2]^+$, respectively. X-ray diffraction studies were performed to determine the coordination pattern in the solid state. In the case of [emim][ClO_4] and [emim][$EtSO_4$], crystal structures confirmed the NMR data, resulting in the complexes $[Li(bipy)_2ClO_4]$ and $[Li(phen)_2EtSO_4]$, respectively. On the contrary, the ionic liquid [emim][NTf_2] generated the C_i symmetric, dinuclear, supramolecular cluster $[Li(bipy)(NTf_2)]_2$, where the individual Li^+ centers were found to be bridged by two [NTf_2] anions. Density functional theory (DFT)-calculations lead to further information on the effect of stacking on the coordination geometry of the Li^+ centers.

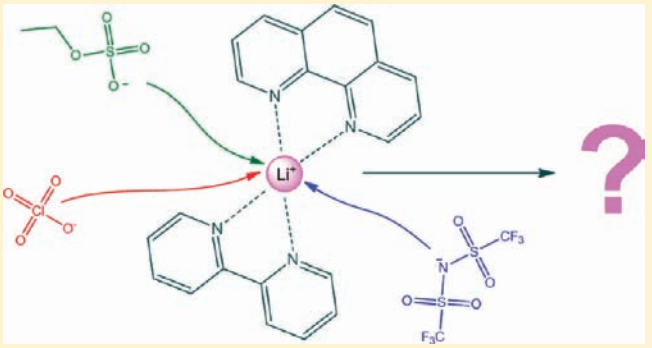

INTRODUCTION

In recent years, the demand for environmental friendly and sustainable chemistry has led to a deeper interest in solvent effects and the search for customized, so-called designer solvents.[1,2] As a result of their tunable properties, such as density, viscosity, polarity, conductivity, and melting point, room temperature ionic liquids (RTILs) have emerged as one of the most promising approaches, and their application has already been well established in new technologies.[3] However, since ILs only consist of cations and anions, they provide a completely different chemical environment as compared to conventional, molecular solvents. This raises the question of how dissolved substrates actually interact with this unique environment, and whether ILs do more than simply behave as another solvent.

In terms of the nucleophilicity of the different anions that form part of the ILs, for example, Cl^-, Br^-, SCN^-, NO_3^-, and $N(CN)_2^-$, most of these anions can act as a Lewis base and coordinate to dissolved metal ions and complexes, either by occupying a vacant coordination site or, if the anion is a strong nucleophile, by displacing weaker bound ligands. This can lead to a significant modification of the metal complex when a labile coordination site that is important for the binding of a substrate, can partially or completely be blocked by the IL anion. Especially the application of sensitive catalytically active metal complexes can therefore be influenced or controlled by interactions with the anionic component of an IL.[4,5] Most recently, Shirai and Ikeda reported on the macrocyclic complexation of Li^+ by the cryptand C211 in ILs as solvents. Compared to the results obtained for nonaqueous solvents, line broadening experiments on the appropriate ^{7}Li NMR signals revealed a mechanistic changeover that could be attributed to the influence of the IL anions.[6]

A detailed knowledge of the possible coordination modes of lithium ions is an essential prerequisite in the development of lithium batteries. Therefore, not only solid electrolytes[7] but also the combination of lithium salts and ILs are of interest.[8−10]

On the basis of our earlier studies on the coordination of lithium ions by bidentate N-donor ligands,[11,12] and our general interest in the effect of ILs[13] used as solvents, it was our aim to investigate the influence of some selected ILs on the formation of such model complexes. In addition, we tried to generate the structural motif $Li[bipy]_3^+$ as found by Hummel et al.[14] by employing ILs in which the anion was systematically varied. We, therefore, selected the ILs 1-ethyl-3-methyl-imidazolium bis(trifluoromethylsulfonyl)imide ([emim][NTf_2]), 1-ethyl-3-methylimidazolium ethylsulfate ([emim][$EtSO_4$]), and 1-ethyl-3-methylimidazolium

Received: March 23, 2011
Published: June 13, 2011

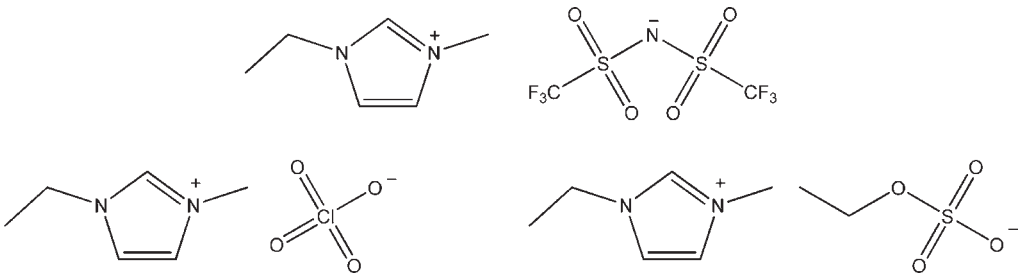

Figure 1. Structures of the ILs [emim][NTf_2], [emim][ClO_4], and [emim][$EtSO_4$].

perchlorate ([emim][ClO_4]) (see Figure 1). The latter was used for the very first time for studies in coordination chemistry. Depending on their solubility in the applied IL, the bidentate N-donor ligands 2,2′-bipyridine (bipy) and 1,10-phenanthroline (phen) were used for the complex-formation reactions of Li^+. To determine the coordination number in solution, the chemical shift of the ^{7}Li NMR signal (abundance: 92.6%) was studied as a function of the added ligand concentration in reference to an external standard. Because different equilibria between solvent molecules, ligands, and metal ions can generate structural motifs in solution that can differ from those derived from crystal structures, we also applied X-ray diffraction to gain more insight into the coordination pattern in the solid state. In addition, quantum chemical calculations were performed to obtain further support for the interpretation of the experimental results.

EXPERIMENTAL SECTION

Materials. All chemicals used in this study were of analytical reagent grade or of the highest purity commercially available. 2,2′-Bipyridine, 1,10-phenanthroline, and lithium perchlorate were purchased from Sigma-Aldrich and used as received. Lithium ethylsulfate was obtained as a side product in the synthesis of the IL [emim][ClO_4] as described below. Lithium bis(trifluoromethysulfonyl)imide and 1-ethyl-3-methylimidazolium bromide were obtained from Iolitec. 1-Ethyl-3-methylimidazolium ethylsulfate was received from Solvent Innovation/Merck and purified as described below. All chemicals were stored under nitrogen atmosphere.

Synthesis of [emim][NTf_2]. To achieve a high purity, contaminations of methylimidazole were removed by repeated recrystallization of [emim]Br from a mixture of methanol and acetone. In this recrystallization procedure [emim]Br was dissolved in an approximately 10% amount of methanol at 65 °C. After cooling to room temperature, precooled acetone was added in a ratio of 1:1 compared to [emim]Br. Crystallization occurred overnight at a temperature of −23 °C. [emim][NTf_2] was synthesized from [emim]Br and Li[NTf_2] by anion metathesis, as described elsewhere.[15] The water content was found to be 0.00% after drying under high vacuum for 5 days, at 50 °C. Elemental Analysis calculated (%) for $C_8H_{11}F_6N_3O_4S_2$: C, 24.55; H, 2.83; N, 10.74; S, 16.39; found: C, 24.78; H, 2.65; N, 10.92; S, 16.54.

Purification of [emim][$EtSO_4$]. Traces of impurities were removed by repeated extraction with a mixture of dichloromethane and water in a volume ratio of 1:1. To achieve a higher optical purity, [emim][$EtSO_4$] was stirred for one week with activated charcoal (Acros Organics: Norit A SUPRA) under high vacuum at a temperature of 55 °C. After filtration with a Millipore filter, Ø = 0.2 μm, the water content was determined by Karl Fischer titration and found to be 0.03%. Elemental Analysis calculated (%) for $C_8H_{16}N_2O_4S$: C, 40.66; H, 6.83; N, 11.86; S, 13.57; found: C, 40.55; H, 6.66; N, 12.13; S, 13,24.

Synthesis of [emim][ClO_4]. The IL [emim][ClO_4] was prepared from $LiClO_4$ and [emim][$EtSO_4$] according to the direct anion metathesis procedure, described elsewhere.[16] Li[$EtSO_4$] was thereby generated as the corresponding side product. After removal of the applied solvent mixture and drying under high vacuum, [emim][ClO_4] was obtained as a clear, colorless liquid in a yield of 94% with a water content of 0.02%. Elemental Analysis calculated (%) for $C_6H_{11}ClN_2O_4$: C, 34.22; H, 5.26; N, 13.30; found: C, 34.22; H, 5.50; N, 13.15.

Synthesis of [Li(bipy)(NTf_2)]$_2$ (1). Solid bipy (234 mg; 1.5 mmol) was added under argon atmosphere to a solution of Li[NTf_2] (144 mg; 0.5 mmol) in 3 mL of [emim][NTf_2]. The reaction mixture was heated to 60 °C under stirring to dissolve the solid bipy. Subsequently, the mixture was stored in the refrigerator at 3 °C. Within several days colorless crystals appeared. Elemental Analysis calculated (%) for $C_{24}H_{16}F_{12}Li_2N_6O_8S_4$: C, 32.51; H, 1.82; N, 9.48 S, 14.47; found: C, 32.01; H, 1.45; N, 9.36; S, 14.89.

Synthesis of 3[Li(bipy)$_2$$ClO_4$]·0.5 bipy (2). Solid bipy (234 mg; 1.5 mmol) was added to a solution of Li[ClO_4] (53 mg; 0.5 mmol) in 3 mL of [emim][ClO_4]. The reaction mixture was heated to 60 °C under stirring to dissolve the solid bipy. Subsequently, the mixture was stored in the refrigerator at 3 °C. Within several days colorless crystals appeared. Elemental Analysis calculated (%) for $C_{65}H_{52}Cl_3Li_3N_{13}O_{12}$: C, 58.53; H, 3.93; N, 13.65; found: C, 57.94; H, 3.82; N, 13.44.

Synthesis of [Li(phen)$_2$($EtSO_4$)] (3). Solid phen (270 mg; 1.5 mmol) was added to a solution of Li[$EtSO_4$] (66 mg; 0.5 mmol) in 3 mL of [emim][$EtSO_4$]. The reaction mixture was heated to 60 °C under stirring to dissolve the solid phen. Subsequently, the mixture was stored in the refrigerator at 3 °C. Within several days colorless crystals appeared. Elemental Analysis calculated (%) for $C_{26}H_{21}LiN_4O_4S$: C, 63.41; H, 4.30; N, 11.38; S, 6.51; found: C, 62.45; H, 4.25; N, 11.16 S, 6.50.

Elemental Analyses. Elemental Analysers (Euro EA 3000 (Euro Vector) and EA 1108 (Carlo Erba)) were used for chemical analyses.

NMR Sudies. All operations were performed under nitrogen atmosphere by use of standard Schlenk techniques. In a typical series of measurements, a solution of bipy or phen (1.0 M in the IL) was mixed in different volume ratios with a 0.05 M solution of the appropriate lithium salt. In each case 540 μL of the lithium-ligand solution mixture was transferred under nitrogen atmosphere to a NMR tube, and a glass capillary (Ø = 1 mm) filled with an external standard (0.1 M $LiClO_4$ solution in DMF) was placed inside the NMR tube. The ^{7}Li NMR spectra were recorded at a frequency of 155 MHz on a Bruker Avance DRX 400WB spectrometer equipped with a superconducting BC-94/89 magnet system. All measurements were performed at room temperature under ambient pressure.

X-ray Crystal Structure Determination. Intensity data were collected either on a Bruker-Nonius KappaCCD diffractometer ([Li(bipy)(NTf_2)]$_2$ and [Li(phen)$_2$($EtSO_4$)]) or on a Bruker Smart APEX-II diffractometer (3[Li(bipy)$_2$$ClO_4$]·0.5 bipy) using graphite monochromatized Mo$K\alpha$ radiation (λ = 0.71073 Å). Data were corrected for Lorentz and polarization effects, and semiempirical absorption corrections were performed on the basis of multiple scans using SADABS.[17] All structures were solved by direct methods and refined by full-matrix least-squares procedures on F^2 using SHELXTL NT 6.12.[18] All non-hydrogen

dx.doi.org/10.1021/ic200594e |*Inorg. Chem.* 2011, 50, 6685–6695

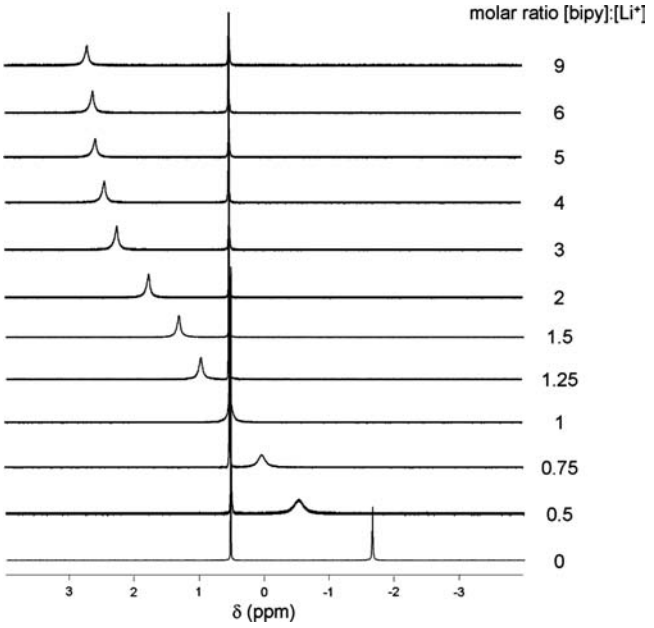

Figure 2. ^{7}Li NMR spectra recorded as a function of the molar ratio [bipy]:[Li^+] in [emim][NTf_2] at 25 °C; Li[NTf_2] was used as a source of Li^+ ions.

atoms were refined with anisotropic displacement parameters. The hydrogen atoms were placed in positions of optimized geometry, and their isotropic displacement parameters were tied to those of the corresponding carrier atoms by a factor of 1.2 or 1.5.

Quantum-Chemical Calculations. All structures were fully optimized using the B3LYP hybrid density functional[19] and LANL2DZ[20] basis set augmented with polarization functions (further denoted as LANL2DZp).[21,22] All structures were characterized as minima by computation of vibrational frequencies. The GAUSSIAN 03 suite of programs was used throughout.[23]

RESULTS AND DISCUSSION

^{7}Li NMR Studies. On the basis of our earlier studies,[11] the number of bidentate ligand molecules coordinated to a Li^+ ion in solution was determined by applying ^{7}Li NMR measurements. In a typical experiment the concentration of the appropriate lithium salt was kept constant, while the concentration of the bidentate ligand was varied over a wide range. The resulting chemical shift of the ^{7}Li signal was then plotted against the mole ratio of [ligand]:[Li^+]. When such a plot shows a remarkable discontinuity in the chemical shift, the appropriate [ligand]:[Li^+] ratio can be taken as the coordination number relative to the bidentate ligand.[24] Although such experiments can not reveal unequivocal information to which extent the remaining coordination site is indeed occupied by an anion of the employed IL, we can at least estimate whether the first coordination sphere provides enough space for the coordination of a solvent anion. On the basis that a maximum of three phen or bipy molecules can occupy six coordination sites as found by Hummel et al,[14] we can then estimate the number of remaining vacant coordination sites.

Coordination of Li^+ by bipy in [emim][NTf_2]. The bis(trifluoromethylsulfonyl)imide anion (NTf_2^-) is one of the most common building blocks used in ILs. On the one hand many ILs that contain this anion have melting points below 0 °C and low viscosities, whereas on the other hand the NTf_2^- anion exhibits a weak coordinating ability because of its sterically

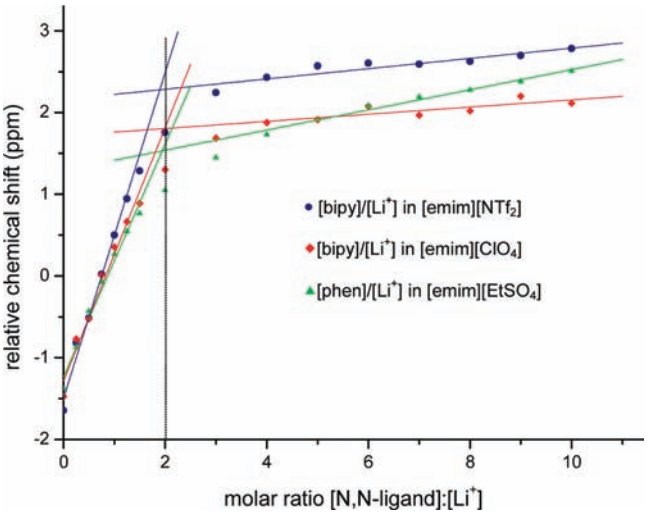

Figure 3. Chemical shift of the ^{7}Li signal as a function of the molar ratio [*N*,*N*-ligand]:[Li^+] at 25 °C.

demanding and electron withdrawing trifluoromethyl groups. Thus, we started our investigations on the coordination of bipy to Li^+ ions, using the IL [emim][NTf_2] (Guttmann Donor Number DN = 11.2 kcal/mol)[25] as solvent. To avoid effects of other anions, Li[NTf_2] was employed as a source for Li^+ ions.

As illustrated by the NMR spectra in Figure 2, the successive addition of bipy leads to a significant downfield shift of the ^{7}Li signal up to a molar ratio of about [bipy]:[Li^+] = 4:1, suggesting a strong interaction between Li^+ and bipy. At higher concentration levels of bipy, the ^{7}Li signal is only slightly further shifted and the first coordination sphere of the Li^+ center is almost saturated. In Figure 3 the chemical shift was plotted as a function of the molar ratio [bipy]:[Li^+], and the straight lines (blue color) clearly indicate a break point in the chemical shift at a molar ratio of [bipy]:[Li^+] = 2:1. This suggests that under these conditions two bipy molecules occupy the first coordination sphere of the Li^+ ion. As a result of the curvature observed in the data, the measured chemical shift at this ratio is not identical to the value expected from the crossing point of the straight lines. Therefore, the equilibrium between nonchelated and chelated Li^+ has to be formulated according to eq 1.

$$Li^+ + 2N,N\text{-ligand} \rightleftharpoons [Li(N,N\text{-ligand})_2]^+ \qquad (1)$$

To clarify whether the first coordination sphere of the Li^+ center is occupied by an additional anion of the employed IL, we also investigated the possible coordination of NTf_2^- using nitromethane as solvent. Here the successive addition of [emim][NTf_2] to a solution of $LiClO_4$ in nitromethane led to a small upfield shift of the ^{7}Li signal, indicating that only weak interactions between Li^+ and NTf_2^- are present (Supporting Information, Figure S1). Nevertheless, a clear discontinuity in the chemical shift is observed for a molar ratio of [NTf_2^-]:[Li^+] = 2:1, suggesting the coordination of two NTf_2^- anions.[26] On the basis of results from other groups, it seems plausible to expect coordination of NTf_2^- in the η^2-mode via the sulfonyl oxygen atoms, which leads to an overall tetrahedral coordination geometry of the Li^+ center.[27] Thus, the formation of $[Li(bipy)_2]^+$ occurs via displacement of coordinated NTf_2^- by bipy, and the occupation of

Table 1. Overall Stability Constants β_2 for Li(*N*,*N*-ligand)$_2$ Complexes

complex	solvent	donor number [kcal/mol]	β_2 [M^{-2}]	log β_2	log β_2 (literature)
Li(bipy)$_2$	[emim][NTf_2]	11.2	$(29 \pm 3) \times 10^3$	4.46	
Li(bipy)$_2$	[emim][ClO_4]	7.6	$(28 \pm 3) \times 10^3$	4.45	
Li(phen)$_2$	[emim][$EtSO_4$]	22.3	$(21 \pm 1) \times 10^3$	4.32	
Li(bipy)$_2$	nitromethane	2.7	$(57 \pm 8) \times 10^3$ [a]	4.76	4.73 (ref 32)
Li(phen)$_2$	nitromethane	2.7	$(153 \pm 38) \times 10^3$ [a]	5.18	

[a] These values were derived from the data presented in ref 11.

further coordination sites by an additional anion can therefore be excluded.

Coordination of Li^+ by bipy in [emim][ClO_4]. The tetrafluoroborate anion (BF_4^-) is one of the anions with the lowest coordinating ability suitable for the synthesis of RTILs. However, the application of BF_4^- can be very problematic because of its hydrolytic sensitivity. Perchlorate anions (ClO_4^-) exhibit a low polarizability and also behave as poor nucleophiles because of a complete delocalization of their negative charge over four oxygen atoms. In combination with the [emim] cation they also generate a RTIL with a Donor Number of 7.6 kcal/mol, which is quite similar to that of [emim][BF_4] (DN = 7.3 kcal/mol).[25] We, therefore, also studied the influence of the weakly coordinating RTIL [emim][ClO_4] on the complexation of Li^+ by bipy. Similar to the NMR data obtained for [emim][NTf_2], the stepwise addition of bipy to a solution of $LiClO_4$ led to a significant downfield shift of the ^{7}Li signal up to a molar ratio of about [bipy]:[Li^+] = 4:1. Above this ratio, higher concentrations of bipy have only little influence on the chemical shift, even though a slightly stronger increase is observed as compared to [emim][NTf_2]. This can be ascribed to a stronger competition between bipy and ClO_4^-, which exhibits less sterical hindrance than NTf_2^- because of its smaller molecular size. Nevertheless, the first coordination sphere of the Li^+ ions is almost saturated and complexation by bipy is clearly favored. As outlined by the crossing point of the red lines (see Figure 3) a significant discontinuity in the chemical shift is observed for a molar ratio of [bipy]:[Li^+] = 2:1, which suggests the coordination of two bipy molecules to a Li^+ ion. Because of its low coordinating ability, we were not able to determine the coordination mode of ClO_4^- anions to Li^+ by NMR studies. Further performed ^{17}O and ^{35}Cl NMR measurements only exhibited single signals that were not very informative. Although most studies on related systems indicate that Li^+ is 4-fold coordinated in solution,[28] Wickleder and Henderson et al. published a crystal structure[29] that exhibits Li^+ ions coordinated in an octahedral mode by η^1 bound ClO_4^- anions. Therefore, we can not completely exclude additional coordination of a maximum of two ClO_4^- anions within the first coordination sphere.

Coordination of Li^+ by phen in [emim][$EtSO_4$]. The direct alkylation of 1-methylimidazole with diethylsulfate is an effective, halide free synthesis, and the resulting IL [emim][$EtSO_4$] is one of the cheapest ILs commercially available.[30] In addition, [emim][$EtSO_4$] can be used as a source of [emim] cations in the synthesis of other ILs by applying direct or membrane assisted metathesis procedures.[31] Although [emim][$EtSO_4$] exhibits a Gutmann Donor Number of 22.3 kcal/mol and the ethylsulfate anion is supposed to coordinate to lithium ions,[25] it was quite interesting to see whether this cheap but coordinating IL influences or even prevents complex-formation reactions.

We used phen instead of bipy because of the poor solubility of the latter in [emim][$EtSO_4$]. Despite the fact that phen exhibits a more rigid structure than bipy, earlier studies performed in nitromethane as solvent showed no influence on the coordination behavior and complex-formation reaction.[11] Accordingly, the successive addition of phen to a solution of Li[$EtSO_4$] also leads to large downfield shifts in the ^{7}Li signal. The results are presented by the green dots in Figure 3. Compared to the data obtained for the other solvents, this NMR titration features a more distinct curvature and the ^{7}Li signal at higher ratios than [phen]:[Li^+] = 4:1 is also downfield shifted. This leads to the conclusion that the [$EtSO_4$] anion has a much larger influence on Li^+ and saturation of the first coordination sphere is only reached at higher concentration levels of phen because of the competition between $EtSO_4^-$ and phen to bind to Li^+. However, a discontinuity in the chemical shift of the ^{7}Li signal can again be observed for an approximate ratio of [phen]:[Li^+] = 2:1, as indicated by the red lines in Figure 3. Therefore, complex-formation is not prevented by $EtSO_4^-$, and lithium ions are coordinated by two phen ligands similar to the other systems reported above. Unfortunately, we were again not able to find evidence for the additional coordination of an $EtSO_4^-$ anion. Application of a ^{7}Li NMR titration in a weakly coordinating solvent like nitromethane, led to the precipitation of Li[$EtSO_4$] as a white solid. ^{17}O NMR measurements performed directly on [emim][$EtSO_4$] only showed one broad signal that was not very informative. Thus, the coordination of an additional $EtSO_4^-$ anion can not be completely excluded.

Stability Constants. As mentioned above, the results presented in Figure 3 indicate a clear curvature of the graphs which can be accounted for by an equilibrium (eq 1) between chelated and free lithium ions in solution. Depending on the position of this equilibrium, the observed NMR data differ from the applied linear fits, especially in the region of the observed discontinuity. These differences allow the estimation of the overall stability constants β_2 of the generated $[Li(bipy)_2]^+$ or $[Li(phen)_2]^+$ complexes, by application of eq 2 at a molar ratio [*N*,*N*-ligand]:[Li^+] = 2:1. The appropriate concentrations of free ligand, free lithium and chelated lithium can be calculated from the observed and expected chemical shifts and the total concentrations of Li^+ and *N*,*N*-ligand at this molar ratio, respectively.

$$\beta_2 = \frac{[\mathrm{Li}(N,N\text{-ligand})_2]}{[\mathrm{Li}^+_{\mathrm{free}}][N,N\text{-ligand}_{\mathrm{free}}]^2} \qquad (2)$$

The resulting stability constants β_2 are summarized in Table 1 and compared to data obtained for nitromethane as solvent. In terms of the applied ILs, [emim][NTf_2] and [emim][ClO_4] with a low coordinating ability lead to similar stability constants. Though [emim][NTf_2] exhibits a slightly higher Donor Number,

Table 2. Crystallographic Data, Data Collection, and Refinement Details for the Investigated Compounds

CSD-ref code	CCDC-810346	CCDC-810347	CCDC-810348
substance	$[Li(bipy)(NTf_2)]_2$ (**1**)	$3[Li(bipy)_2ClO_4]\cdot 0.5$ bipy (**2**)	$[Li(phen)_2(EtSO_4)]$ (**3**)
empirical formula	$C_{24}H_{16}F_{12}Li_2N_6O_8S_4$	$C_{65}H_{52}Cl_3Li_3N_{13}O_{12}$	$C_{26}H_{21}LiN_4O_4S$
mol. weight [g/mol]	886.55	1334.37	492.47
crystal size [mm]	0.24 × 0.20 × 0.17	0.45 × 0.28 × 0.18	0.34 × 0.23 × 0.14
temperature [K]	150(2)	100(2)	150(2)
crystal system	triclinic	triclinic	monoclinic
space group	$P\bar{1}$ (no. 2)	$P\bar{1}$ (no. 2)	$P2_1/c$ (no. 14)
a [Å]	9.0329(3)	10.6247(2)	16.7031(10)
b [Å]	9.6847(7)	15.5181(2)	11.1598(6)
c [Å]	10.9049(11)	19.4551(3)	13.2751(7)
α [deg]	68.141(7)	82.158(1)	90
β [deg]	76.947(4)	89.379(1)	107.738(6)
γ [deg]	80.558(5)	77.308(1)	90
V [Å^3]	859.13(11)	3099.41(9)	2356.9(2)
Z	1	2	4
ρ [g/cm^3] (calc.)	1.714	1.430	1.388
μ [mm^{-1}]	0.397	0.224	0.179
F (000)	444	1378	1024
abs. corr	SADABS	SADABS	SADABS
T_{min}; T_{max}	0.804; 0.935	0.662; 0.746	0.840; 0.975
2Θ interval [deg]	7.1 ≤ 2Θ ≤ 55.8	5.2 ≤ 2Θ ≤ 55.8	5.9 ≤ 2Θ ≤ 55.8
coll. refl.	26629	49406	72730
indep. refl.	4098	14532	5623
R(int)	0.0382	0.0391	0.0399
obs. refl. [$I \geq 2\sigma(I)$]	3358	11257	4577
no. ref param.	253	865	326
wR_2 (all data)	0.0837	0.1013	0.1215
R_1 [$I \geq 2\sigma(I)$]	0.0338	0.0388	0.0406
GoF F^2	1.024	1.039	1.040
max.; min res. electr. density[e Å^{-3}]	0.375; −0.325	0.315; −0.577	0.459; −0.396

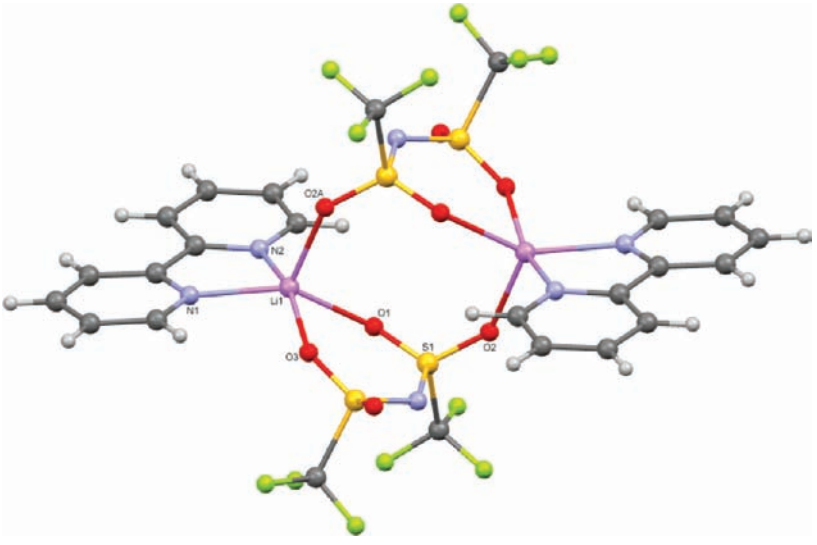

Figure 4. Molecular structure of $[Li(bipy)(NTf_2)]_2$ (**1**).

the larger size of NTf_2^- minimizes interactions with the individual lithium ions, and leads to a slightly higher stability constant compared to $[emim][ClO_4]$. In contrast, $[Li(phen)_2]^+$ exhibits the lowest stability constant. From a comparison of this value with the data derived from nitromethane as solvent, it is obvious that the lack of stability must be attributed to effects of the IL

dx.doi.org/10.1021/ic200594e |*Inorg. Chem.* 2011, 50, 6685–6695

Table 3. Selected Bond Distances [Å] and Bond Angles [deg] of 1

bond	length (meas.)	length (calc.)	bond	angle (meas.)	angle (calc.)
Li(1)−N(1)	2.082(3)	2.12	N(1)−Li(1)−O(1)	146.2(2)	156.8
Li(1)−N(2)	2.077(3)	2.13	O(3)−Li(1)−N(2)	161.8 (2)	151.8
Li(1)−O(1)	2.123(3)	2.07	O(2A)−Li(1)−O(1)	101.5(2)	98.3
Li(1)−O(2A)	2.060(3)	2.03	O(2A)−Li(1)−O(3)	96.0(2)	104.3
Li(1)−O(3)	2.076(3)	2.04	N(2)−Li(1)−O(1)	92.2(2)	92.8

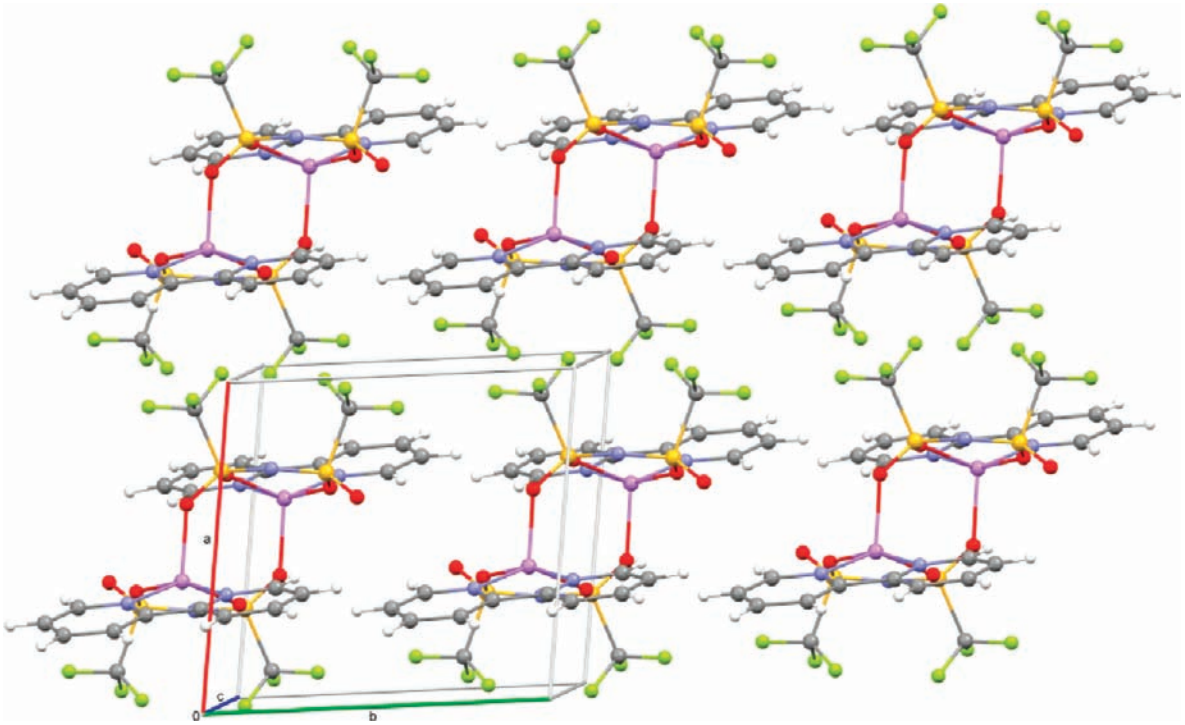

Figure 5. Stacking of **1**; view along the crystallographic **c**-axis.

[emim][$EtSO_4$], as $[Li(phen)_2]^+$ in nitromethane exhibits a significantly higher stability constant than $[Li(bipy)_2]^+$.[32]

X-ray Diffraction Studies. All crystals used for X-ray diffraction studies were obtained directly from the employed ILs. On the basis of our ^{7}Li NMR experiments, we employed lithium salts featuring the same anion as the appropriate IL for crystallization to exclude possible effects of other anions. Important details and parameters concerning the data collection and structure refinements are given in Table 2.

Structure of $[Li(bipy)(NTf_2)]_2$ (1). In contrast to the results obtained from the ^{7}Li NMR experiments, X-ray diffraction studies revealed a completely different coordination pattern of Li^+ in the presence of bipy in the solid state. As shown in Figure 4, the discrete dimeric lithium species $[Li(bipy)(NTf_2)]_2$ (**1**) was found to be the principal structural motif that controls the stacking process. The asymmetric unit of **1** contains one-half of the molecule, whereas the second half is generated by an inversion center, located at the center of the molecule.

Each Li^+ ion is 5-fold coordinated by two nitrogen and three oxygen donor atoms. Following the concept of Addison and Reedijk to characterize the coordination geometry by use of the so-called τ-value ($\tau = (\beta-\alpha)/60$), basal angles of α = 146.17 (16)° (N(1)−Li(1)−O(1)) and β = 161.81 (17)° (O(3)−Li(1)−N(2)) result in a τ value of 0.26. This indicates a distorted square-pyramidal coordination geometry for each Li^+ center.[33] Both bipy and one NTf_2^- anion coordinate in a η^2-mode to a Li^+ ion, spanning the tetragonal base of this polyhedron, whereas the apical position is occupied by an oxygen atom of the second, neighboring NTf_2^- anion. Therefore, the individual Li^+ centers are not only bound η^2 by one NTf_2^- anion. Both Li^+ centers of **1** are in addition bridged by one sulfonyl subunit of each NTf_2^- anion. This leads to a complex structure of two six-membered ring systems connected by an eight-membered ring. Being part of two rings, the distance Li(1)−O(1) (see Table 3) is slightly elongated compared to the other Li−O contacts, indicating a weaker interaction caused by steric effects.

Earlier studies by Davidson et al. on the coordination of tetramethylethylenediamine (TMEDA) led to a similar dimeric lithium species as presented in Figure 4.[34] In contrast to our observations, both Li^+ centers in their structure exhibit trigonal-bipyramidal coordination geometries. By application of density functional theory (DFT) calculations without any symmetry constraints (B3LYP/LANL2DZp), we found that for the TMEDA ligand both structural motifs could be possible (see Supporting Information, Figure S2) and the clear preference for the trigonal-bipyramidal coordination geometry can be attributed to packing effects. However, similar calculations performed on the bipy complex

dx.doi.org/10.1021/ic200594e |*Inorg. Chem.* 2011, 50, 6685–6695

only resulted in a square-pyramidal coordination geometry (α = 151.8°, β = 156.8°, τ = 0.08) (see Table 3 and Supporting Information, Figure S3). This leads to the conclusion that in our case the observed geometry must be favored by a lack of flexibility within the bipy ligand as compared to the TMEDA ligand.

On considering stacking effects, the trifluoromethyl groups of **1** are orientated *cisoid* with respect to the same NTf_2^- anion, whereas those of different anions are found to be *transoid*. As illustrated in Figure 5, **1** is arranged in parallel layers with the trifluoromethyl groups facing other trifluoromethyl groups of the next layer above and below. This leads to the formation of unpolar arrays, the so-called "fluorous regions" that separate the individual layers.[35]

Although the NTf_2^- anion offers different possible ways to coordinate to a metal center (N-donor as well as O-donor), a clear preference for coordination via oxygen atoms is observed.[36,37] This can be ascribed to steric effects, but also be attributed to electronic features. Because of the electron withdrawing character of the trifluoromethyl groups, a large degree of pπ−dπ bonding within the N−S moiety leads to charge delocalization over the whole NTf_2^- anion.[38]

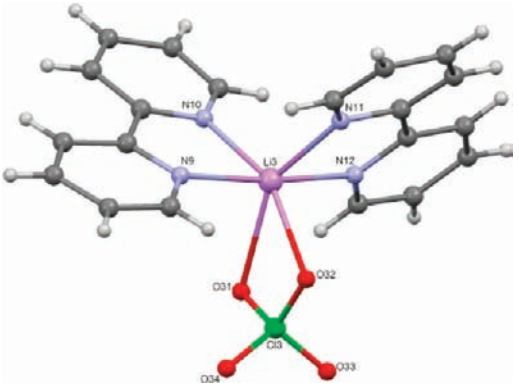

Figure 6. Molecular structure of $Li(bipy)_2ClO_4$ in crystals of **2** (here **Li3**).

Structure of $3[Li(bipy)_2ClO_4]\cdot 0.5$ bipy (2). In agreement with the ^{7}Li NMR data, the single crystal X-ray structure determination revealed a monomeric lithium species with the empirical formula $[Li(bipy)_2ClO_4]$, as shown in Figure 6. Because of additionally enclosed bipy molecules, the crystal structure possesses an asymmetric unit that contains three molecules of

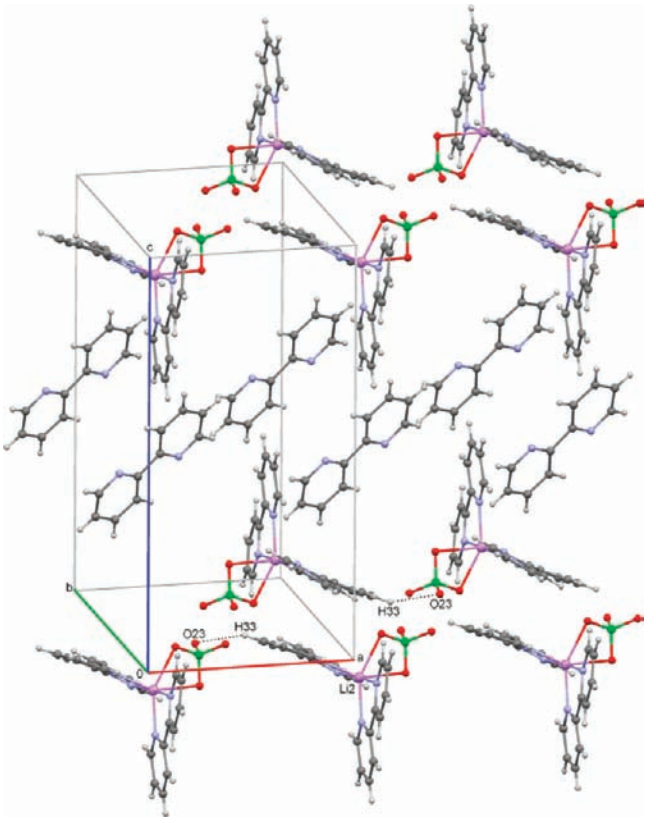

Figure 8. Stacking of **Li2**; view along the crystallographic **b**-axis. **Li1** and **Li3** omitted for clarity.

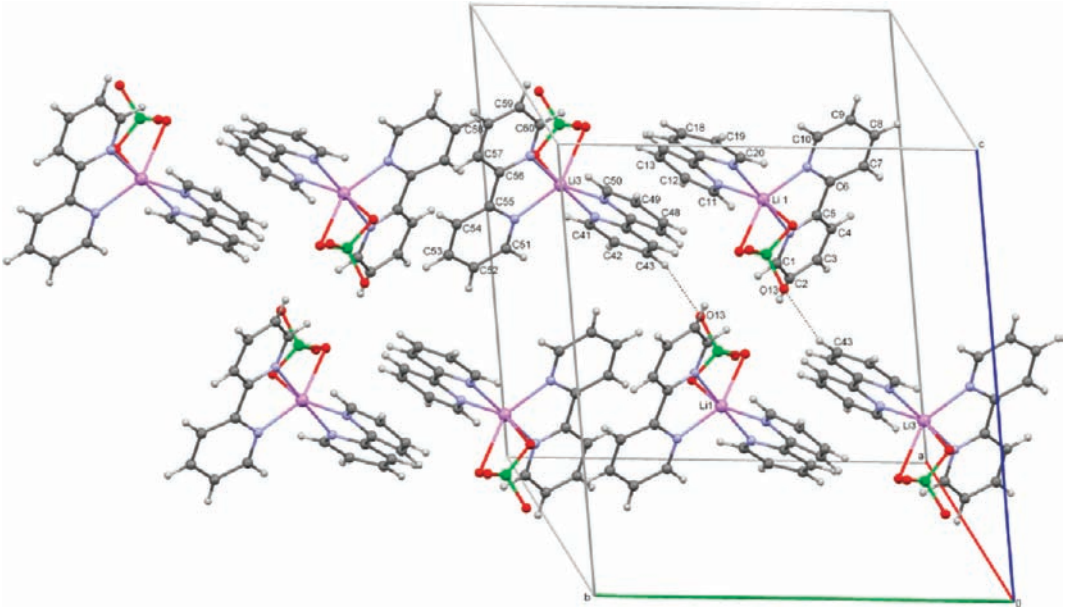

Figure 7. Stacking of **Li1** and **Li3**; view along the crystallographic **a**-axis. **Li2** and additionally enclosed bipy molecules omitted for clarity.

dx.doi.org/10.1021/ic200594e |*Inorg. Chem.* 2011, 50, 6685–6695

$[Li(bipy)_2ClO_4]$ (**Li1**, **Li2**, **Li3**) and a half bipy molecule. Within the asymmetric unit, **Li1**, **Li2**, and **Li3** differ slightly in terms of their bond lengths, bond angles, and torsion angles of the bipy ligands (see Supporting Information, Table S1). However, they all exhibit the same coordination pattern and geometry.

Although ClO_4^- is known to possess a low coordinating ability, the Li^+ center is bound in the η^2-mode by both one ClO_4^- anion and two bipy molecules, leading to a distorted octahedral coordination geometry. On considering the structure of trichelate complexes, bidentate ligands such as bipy, acetylacetone, and so forth are known to form Δ and Λ enantiomers.[39] Surprisingly, we found **Li1**, **Li2**, and **Li3** to be achiral complexes and the bipy moieties to feature torsion angles (N−C−C−N) with different algebraic signs (see Supporting Information, Table S1). To estimate the energy differences between the observed *meso*- and the Δ- or Λ-structures, we tried to calculate (B3LYP/LANL2DZp) the stability of these motifs. However, independent of the starting structure, we only found the chiral motifs to be stable (see Supporting Information, Figure S4). This leads to the conclusion that the achiral structure is preferred as a result of packing effects.

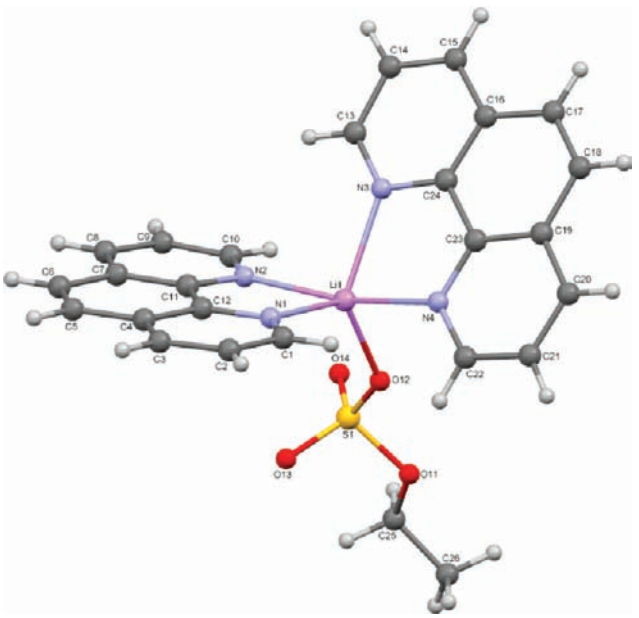

Figure 9. Molecular structure of $[Li(phen)_2(EtSO_4)]$ (**3**).

The crystal structure has several motifs that control the stacking. **Li1** and **Li3** generate two parallel chains that run along the **b**-axis through the center of the unit cell (see Figure 7). Both chains are connected by C−H···O interactions between H(43) and O(13) [C(43)···O(13) = 3.292(2) Å; H(43)···O(13) = 2.41 Å; C(43)−H(43)···O(13) = 154.7°]. Because of an antiparallel arrangement of **Li1** and **Li3** within these chains, the bipy ligands face each other, and the average distances of 3.44 Å (Li1, bipy: N1−C1−C10−N2; Li3, bipy N11−C51−C60−N12, determined as the distance between the centers of the neighbor C6−C7 and C54−C55 bonds) and 3.63 Å (Li1, bipy: N3−C11−C20−N4; Li3, bipy N9−C41−C50−N10, determined as the distance between the centers of the neighbor C15−C16 and C45−C46 bonds) enable $\pi-\pi$ interactions between parts of these ligands. As shown in Figure 8, the **Li2** complexes are located in opposite directions above and below the **ab**-planes, likewise generating two parallel chains but running along the **a**-axis. Within each chain, the individual **Li2** complexes are connected by C−H···O interactions between H(33) and O(23) of the next complex [C(33)···O(23) = 3.390(2) Å; H(33)···O(23) = 2.52 Å; C(33)−H(33)···O(23) = 152.5°]. Because of the symmetry, the bipy ligands (N7−C31−C40−N8) face each other and the average distances of 3.44 Å (determined as the distance between the

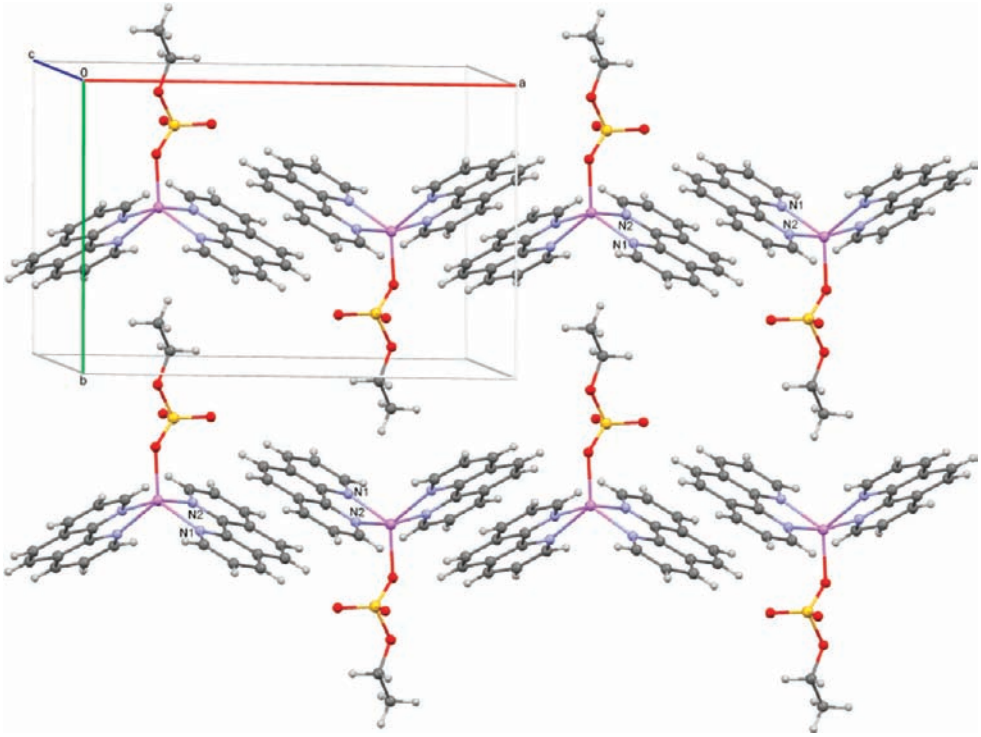

Figure 10. Stacking of **3**; view along the crystallographic **c**-axis (top view on a monolayer).

dx.doi.org/10.1021/ic200594e |*Inorg. Chem.* 2011, 50, 6685–6695

Table 4. Selected Bond Lengths [Å] and Bond Angles [deg] of 3

bond	length (meas.)	length (calc.)	bond	angle (meas.)	angle (calc.)
Li(1)−N(1)	2.121(3)	2.13	N(1)−Li(1)−N(3)	111.1(2)	97.8
Li(1)−N(2)	2.185(3)	2.17	N(4)−Li(1)−N(2)	166.9(2)	165.9
Li(1)−N(3)	2.215(3)	2.35	O(12)−Li(1)−N(1)	121.9(2)	112.8
Li(1)−N(4)	2.160(3)	2.17	O(12)−Li(1)−N(3)	126.8(2)	148.6
Li(1)−O(12)	2.047(3)	1.91	O(12)−Li(1)−N(2)	99.5(2)	99.1

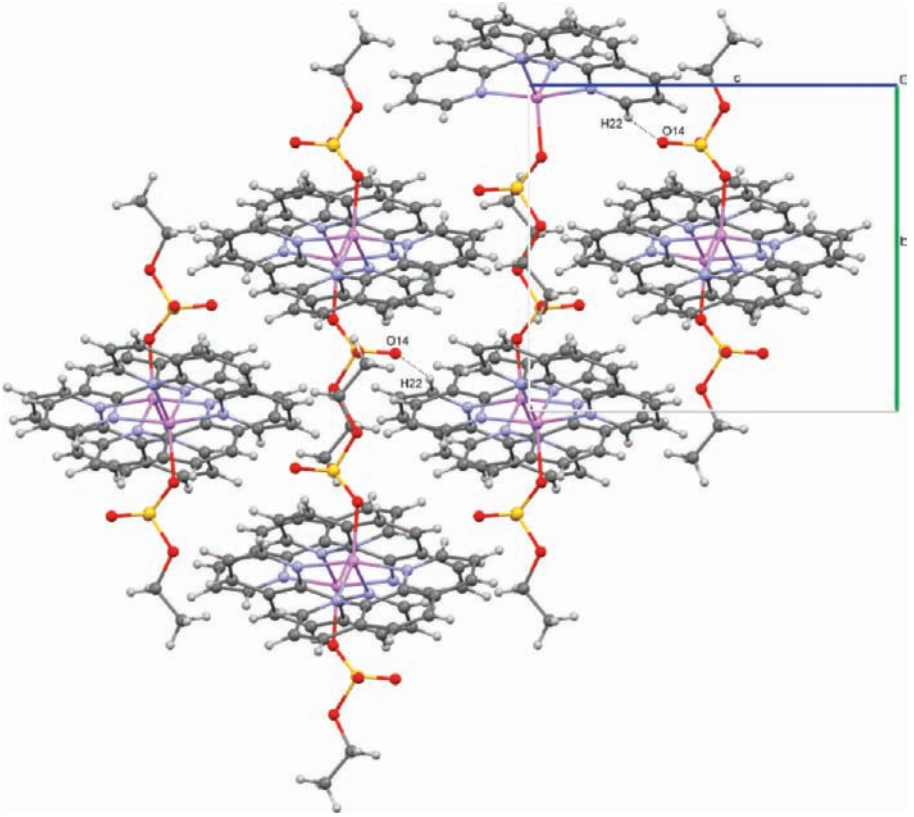

Figure 11. Stacking of **3**; view along the crystallographic **a**-axis.

centers of two neighbor C36−C37 bonds) indicate $\pi-\pi$ interactions through the **ab**-plane that connect both chains.

The structural motifs presented in Figures 7 and 8 cross each other similar to tree trunks of a blockhouse. As mentioned above, the crystal exhibits additionally enclosed bipy molecules, not taking part in any coordination and therefore featuring a more stable *transoid* and nearly planar conformation.[40] These molecules fill the remaining space, that is, in the center of the **c**-axis.

Structure of [Li(phen)$_2$(EtSO$_4$)] (3). As shown in Figure 9, X-ray diffraction studies revealed a monomeric lithium species, being the principal structural motif that exhibits the empirical formula [Li(phen)$_2$(EtSO$_4$)] (**3**). The asymmetric unit of **3** contains the molecule itself.

In agreement with the results obtained from our NMR data, Li^+ ions in the solid state are likewise coordinated by two phen molecules. Together with a monodentate bound $EtSO_4^-$ anion, each Li^+ center is 5-fold coordinated and basal angles of α = 111.09 (13)° (N(1)−Li(1)−N(3)) and β = 166.92 (15)° (N(4)−Li(1)−N(2)) result in a τ value of 0.93, indicating a distorted, trigonal-bipyramidal coordination geometry.[33] The phen molecules occupy in the η^2 mode the axial as well as two equatorial positions, whereas the third equatorial position is bound by one of the terminal oxygen atoms of the $EtSO_4^-$ anion. Although sulfate ions and their derivates exhibit different possible coordination modes (they can behave as monodentate (η^1), bidentate (η^2), or bridging (μ) ligands), structure **3** shows a preference for η^1 coordination. Application of DFT calculations in the absence of symmetry constraints (B3LYP/LANL2DZp) surprisingly led to a 6-fold coordinated Li^+ .species with the $EtSO_4^-$ anion bound in the η^2-mode to the Li^+ center (Supporting Information, Figure S5). A 5-fold coordinated Li^+ complex with the $EtSO_4^-$ anion bound in the η^1-mode was found to be stable if the Li^+ center is included in the square-pyramidal coordination geometry (α = 148.6°, β = 165.9°, τ = 0.29) (Supporting Information, Figure S6). Therefore, the trigonal-bipyramidal constitution of **3** can be attributed to stacking effects that lead to a better $\pi-\pi$ interaction mentioned below.

The stacking can be described by vertical layers consisting of parallel chains running along the crystallographic **a**-axis

dx.doi.org/10.1021/ic200594e |*Inorg. Chem.* 2011, 50, 6685–6695

(Figure 10). Within these chains, compound **3** is arranged antiparallel in a zigzag pattern. Because of the symmetry, phen ligands using the same labeling span parallel planes with a distance of 3.46 Å (phen: N1−C1−C12−N2, determined as the distance between neighbor C4 atoms) and 3.41 Å (phen: N3−C13−C24−N4, determined as the distance between the centers of neighbor C15−C16 and C23−C24 bonds). These distances indicate $\pi-\pi$ interactions between parts of the aromatic phen systems, leading to a shorter Li(1)−N(1) = 2.121(3) Å and a longer Li(1)−N(3) = 2.215(3) Å bond length. Compared to the other Li−N bonds (Table 4), these distances deviate for steric reasons and lead to a better $\pi-\pi$ interaction. As shown in Figure 11, the vertical layers outlined in Figure 10 are successively staggered. This arrangement enables the formation of C−H···O interactions between H(22) and O(14) of the next vertical layer [C(22)···O(14) = 3.242(2) Å; H(22)···O(14) = 2.36 Å; C(22)−H(22)···O(14) = 154.6°] and leads to an interaction of the individual layers over the whole surface.

CONCLUSIONS

The results obtained from our ^{7}Li NMR studies clearly demonstrate that Li^+ ions, diluted in the three employed ILs, are chelated by two bipy or phen molecules. In the case of [emim][ClO_4] and [emim][$EtSO_4$], this observation was confirmed by crystal structures, where each Li^+ center was found to be coordinated by two chelate molecules and one anion of the corresponding solvent. Although the coordination of an anion could be an effect of charge neutralization and therefore an effect of the crystallization process, a likewise coordination of these anions in solution can not be excluded completely. To our surprise, the NTf_2^- anion, which was supposed to have only little influence on the complex-formation reaction, generated a completely different coordination pattern in the solid state. This means that the coordination behavior of the NTf_2^- anion caused by its electronic properties can have a significant influence on the solid state structure, even though NTf_2^- seems to behave nearly innocent in solution. Redissolving these crystals in [emim][NTf_2] must then lead to a different complex structure in solution, because of the new ratio of [bipy]/[Li^+] = 1:1. Despite an excess of bipy or phen over Li^+, the structural motif [Li(bipy)$_3$], as found by Hummel et al.,[14] was not observed in this study, neither in solution nor in the crystal structures. Thus, the generation of this motif must be an effect of their binary melts, since Hummel et al. used bipy itself as solvent. These observations clearly demonstrate that our understanding of how metal salts dissolve in ILs, and how ILs actually interact with catalytically active complexes, remains rather limited. On the other hand the reported molecular and crystal structures of lithium complexes in ILs form a good basis for systematic studies on the chemical reactions of such complexes in ILs.

As a result of decades of research, scientists have developed a good understanding of the role of conventional solvents, but still much more needs to be done to reach such an understanding for the role of ILs as solvents in coordination chemistry.

ASSOCIATED CONTENT

Supporting Information. The chemical shift of the ^{7}Li signal as a function of the added NTf_2^- concentration, the calculated structures (B3LYP/LANL2DZp) of [Li(TMEDA)(NTf_2)]$_2$, [Li(bipy)(NTf_2)]$_2$, [Li(bipy)$_2$$ClO_4$], [Li(phen)$_2$($EtSO_4$)] and a table with selected bond lengths, angles and torsion angles concerning the crystal structure of [Li(bipy)$_2$$ClO_4$]. This material is available free of charge via the Internet at http://pubs.acs.org.

AUTHOR INFORMATION

Corresponding Author
*E-mail: vaneldik@chemie.uni-erlangen.de.

ACKNOWLEDGMENT

The authors gratefully acknowledge financial support from the Deutsche Forschungsgemeinschaft through SPP 1191 (Ionic Liquids).

REFERENCES

(1) *Modern Solvents in organic Synthesis*; Knochel, P., Ed.; Springer-Verlag: Berlin, Germany, 1999.

(2) Adams, D. J.; Dyson, P. J.; Tavener, S. J. In *Chemistry in Alternative Reaction Media*; Wiley: Chichester, England, 2004.

(3) (a) Maase, M. *Multiphase Homogeneous Catal.* **2005**, *2*, 560–566. (b) Tempel, D.; Henderson, P.; Brzozowski, J.; Pearlstein, R.; Garg, D. U.S. Patent Application Publ. 2006, 15 pp Cont.-in-part of U.S. Ser. No. 9482, 277.

(4) (a) Earle, M. J.; Hakala, U.; McAuley, B. J.; Nieuwnhuyzen, M.; Ramani, A.; Seddon, K. R. *Chem Commun.* **2004**, *12*, 1368–1369. (b) Magna, L.; Chauvin, Y.; Niccolai, G. P.; Basset, J. M. *Organometallics* **2003**, *22*, 4418–4425.

(5) (a) Mc. Nulty, J.; Cheekoori, S.; Bender, T. P.; Coggan, J. A. *Eur. J. Org. Chem.* **2007**, *9*, 1423–1428. (b) Daguenet, C.; Dyson, P. *Organometallics* **2006**, *25*, 5811–5816. (c) Schmeisser, M.; van Eldik, R. *Inorg. Chem.* **2009**, *48*, 7466–7475.

(6) Shirai, A.; Ikeda, Y. *Inorg. Chem.* **2011**, *50*, 1619–1627.

(7) (a) Mariappan, C. R.; Govindaraj, G.; Roling, B. *Solid State Ionics* **2005**, *176*, 723–729. (b) Taskiran, A.; Schirmeisen, A.; Fuchs, H.; Bracht, H.; Roling, B. *Phys. Chem. Chem. Phys.* **2009**, *11*, 5499–5505.

(8) Frömling, T.; Kunze, M.; Schönhoff, M.; Sundermeyer, J.; Roling, B. *J. Phys. Chem. B* **2008**, *112*, 12985–12990.

(9) (a) Henderson, W. A.; Brooks, N. R.; Brennessel, W. W.; Young, V. G. *Chem. Mater.* **2003**, *15*, 4679–4684. (b) Henderson, W. A.; Brooks, N. R.; Young, V. G. *Chem. Mater.* **2003**, *15*, 4685–4690. (c) Henderson, W. A.; Passserini, S. *Chem. Mater.* **2004**, *16*, 2881–2885. (d) Castriota, M.; Caruso, T.; Agostino, R. G.; Cazzanelli, E.; Henderson, W. A.; Passserini, S. *J. Phys. Chem. A* **2005**, *109*, 92–96. (e) Henderson, W. A.; McKenna, F.; Khan, M. A.; Brooks, N. R.; Young, V. G.; Frech, R. *Chem. Mater.* **2005**, *17*, 2284–2289. (f) Zhou, Q.; Henderson, W. A.; Appetecchi, G. B.; Passserini, S. *J. Phys. Chem. C* **2010**, *114*, 6201–6204. (g) Zhou, Q.; Fitzgerald, K.; Boyle, P. D.; Henderson, W. A. *Chem. Mater.* **2010**, *22*, 1203–1208.

(10) (a) Henderson, W. A.; Brooks, N. R.; Young, V. G. *J. Am. Chem. Soc.* **2003**, *125*, 12098–12099. (b) Henderson, W. A.; Brooks, N. R.; Brennessel, W. W.; Young, V. G. *J. Phys. Chem. A* **2004**, *108*, 225–229. (c) Andreev, Y. G.; Seneviratne, V.; Khan, M.; Henderson, W. A.; Frech, R. E.; Bruce, P. G. *Chem. Mater.* **2005**, *17*, 767–772. (d) Grondin, J.; Talaga, D.; Lassègues, J.-C.; Henderson, W. A. *Phys. Chem. Chem. Phys.* **2004**, *6*, 938–944. (e) Grondin, J.; Lassègues, J.-C.; Chami, M.; Servant, L.; Talaga, D.; Henderson, W. A. *Phys. Chem. Chem. Phys.* **2004**, *6*, 4260–4267. (f) Henderson, W. A. *J. Phys. Chem. B* **2006**, *110*, 13177–13183.

(11) Schmeisser, M.; Zahl, A.; Scheurer, A.; Puchta, R.; van Eldik, R. *Z. Naturforsch. B* **2010**, *65*, 405–413.

(12) (a) Buttery, J. H. N.; Effendy; Mutrofin, S.; Plackett, N. C.; Skelton, B. W.; Whitaker, C. R.; White, A. H. *Z. Anorg. Allg. Chem.* **2006**, *632*, 1809–1828. (b) Buttery, J. H. N.; Effendy; Koutsantonis, G. A.;

Mutrofin, S.; Plackett, N. C.; Skelton, B. W.; Whitaker, C. R.; White, A. H. *Z. Anorg. Allg. Chem.* **2006**, *632*, 1829–1838. (c) Buttery, J. H. N.; Effendy; Mutrofin, S.; Plackett, N. C.; Skelton, B. W.; Somers, N.; Whitaker, C. R.; White, A. H. *Z. Anorg. Allg. Chem.* **2006**, *632*, 1839–1850. (d) Buttery, J. H. N.; Effendy; Koutsantonis, G. A.; Mutrofin, S.; Plackett, N. C.; Skelton, B. W.C.; Whitaker, R.; White, A. H. *Z. Anorg. Allg. Chem.* **2006**, *632*, 1850–1855.

(13) Hubbard, C. D.; Illner, P.; van Eldik, R. *Chem. Soc. Rev.* **2011**, *40*, 272–290.

(14) Fischer, E.; Hummel, H.-U. *Z. Anorg. Allg. Chem.* **1997**, *623*, 483–486.

(15) Bonhôte, P.; Dias, A.-P.; Papageorgiou, N.; Kalyanasundaram, K.; Grätzel, M. *Inorg. Chem.* **1996**, *35*, 1168–1178.

(16) Schmeisser, M. et al., manuscript in preparation.

(17) *SADABS 2.06*, Bruker AXS, Inc. 2002, Madison, WI, USA and *SADABS 2008/1*, Bruker AXS, Inc. 2008, Madison, WI, USA.

(18) *SHELXTL NT*, 6.12; Bruker AXS, Inc.: Madison, WI, 2002.

(19) (a) Becke, A. D. J. *Chem. Phys.* **1993**, *98*, 5648–5652. (b) Lee, C.; Yang, W.; Parr, R. G. *Phys. Rev. B* **1988**, *37*, 785–789. (c) Stephens, P. J.; Devlin, F. J.; Chabalowski, C. F.; Frisch, M. J. J. *Phys. Chem.* **1994**, *98*, 11623–11627.

(20) (a) Hay, P. J.; Wadt, W. R. *J. Chem. Phys.* **1985**, *82*, 270–283. (b) Hay, P. J.; Wadt, W. R. *J. Chem. Phys.* **1985**, *82*, 284–298. (c) Hay, P. J.; Wadt, W. R. *J. Chem. Phys.* **1985**, *82*, 299–310.

(21) Huzinaga, S.; Andzelm, J.; Klobukowski, M.; Radzi-Andzelm, E.; Sakai; Y.; Tatewaki, H. In *Gaussian Basis Sets for Molecular Calculations*; Elsevier: Amsterdam, The Netherlands, 1984.

(22) The performance of this method is well documented, see for example: (a) Illner, P.; Zahl, A.; Puchta, R.; van Eikema Hommes, N.; Wasserscheid, P.; van Eldik, R. *J. Organomet. Chem.* **2005**, *690*, 3567–3576. (b) Puchta, R.; Meier, R.; van Eikema Hommes, N.; van Eldik, R. *Eur. J. Inorg. Chem.* **2006**, *20*, 4063–4067. (c) Puchta, R.; Meier, R.; van Eldik, R. *Aust. J. Chem.* **2007**, *60*, 889–897. (d) Illner, P.; Puchta, R.; Heinemann, F. W.; van Eldik, R. *Dalton Trans.* **2009**, *15*, 2795–2801. (e) Soldatović, T.; Shoukry, M.; Puchta, R.; Bugarčić, Ž. D.; van Eldik, R. *Eur. J. Inorg. Chem.* **2009**, *15*, 2261–2270.

(23) Frisch, M. J.; Trucks, G. W.; Schlegel, H. B.; Scuseria, G. E.; Robb, M. A.; Cheeseman, J. R.; Montgomery, Jr., J. A.; Vreven, T.; Kudin, K. N.; Burant, J. C.; Millam, J. M.; Iyengar, S. S.; Tomasi, J.; Barone, V.; Mennucci, B.; Cossi, M.; Scalmani, G.; Rega, N.; Petersson, G. A.; Nakatsuji, H.; Hada, M.; Ehara, M.; Toyota, K.; Fukuda, R.; Hasegawa, J.; Ishida, M.; Nakajima, T.; Honda, Y.; Kitao, O.; Nakai, H.; Klene, M.; Li, X.; Knox, J. E.; Hratchian, H. P.; Cross, J. B.; Bakken, V.; Adamo, C.; Jaramillo, J.; Gomperts, R.; Stratmann, R. E.; Yazyev, O.; Austin, A. J.; Cammi, R.; Pomelli, J. W. Ochterski, P. Y. Ayala, K. Morokuma, G. A. Voth, P. Salvador, J. J. Dannenberg, V. G. Zakrzewski, S. Dapprich, C.; Daniels, A. D.; Strain, M. C.; Farkas, O.; Malick, D. K.; Rabuck, A. D.; Raghavachari, K.; Foresman, J. B.; Ortiz, J. V.; Cui, Q.; Baboul, A. G.; Clifford, S.; Cioslowski, J.; Stefanov, B. B.; Liu, G.; Liashenko, A.; Piskorz, P.; Komaromi, I.; Martin, R. L.; Fox, D. J.; Keith, T.; Al-Laham, M. A.; Peng, C. Y.; Nanayakkara, A.; Challacombe, M.; Gill, P. M. W.; Johnson, B.; Chen, W.; Wong, M. W.; Gonzalez, C.; Pople, J. A. *GAUSSIAN 03*, Revision C.02; Gaussian, Inc.: Wallingford, CT, 2004.

(24) Schmidt, E.; Hourdakis, A.; Popov, A. I. *Inorg. Chim. Acta* **1981**, *52*, 91–95.

(25) Illner, P.; Puchta, R.; Schmeisser, M.; van Eldik, R., manuscript in preparation.

(26) Nicotera, I.; Oliviera, C.; Henderson, W. A.; Appetecchi, G. B.; Passerini, S. *J. Phys.Chem. B* **2005**, *109*, 22814–22819.

(27) (a) Lassègues, J.; Grondin, T.; Talaga, D. *Phys. Chem. Chem. Phys.* **2006**, *8*, 5629–5632. (b) Umebayashi, Y.; Mitsugi, T.; Fukuda, S.; Fujimori, T.; Fujii, K.; Kanzaki, R.; Takeuchi, M.; Ishiguro, S. *J. Phys Chem. B* **2007**, *111*, 13028–13032.

(28) (a) Pasgreta, E.; Puchta, R.; Galle, M.; van Eikemma-Hommes, N.; Zahl, A.; van Eldik, R. *ChemPhysChem* **2007**, *8*, 1315–1320. (b) Pasgreta, E.; Puchta, R.; Zahl, A.; van Eldik, R. *Eur. J. Inorg. Chem.* **2007**, *13*, 1815–1822.

(29) (a) Wickleder, M. S. *Z. Anorg. Allg. Chem.* **2003**, *629*, 1466–1468. (b) Henderson, W. A.; Brooks, N. R. *Inorg. Chem.* **2003**, *42*, 4522–4524.

(30) Holbrey, J. D.; Reichert, W. M.; Swatloski, R. P.; Broker, G. A.; Pitner, W. R.; Seddon, K. R.; Rogers, R. D. *Green Chem.* **2002**, *4*, 407–413.

(31) Himmler, S.; Koenig, A.; Wasserscheid, P. *Green Chem.* **2007**, *9*, 935–942.

(32) Ghasemi, J.; Shamsipur, M. *Polyhedron* **1996**, *15*, 3647–3652.

(33) Addison, A. W.; Rao, T. N.; Reedijk, J.; van Rijn, J.; Verschoor, G. C. *Dalton Trans.* **1984**, *7*, 1349–1356.

(34) Davidson, M. G.; Raithby, P. R.; Johnson, A. L.; Bolton, P. D. *Eur. J. Inorg. Chem.* **2003**, *18*, 3445–3452.

(35) Holbrey, J. D.; Reichert, W. M.; Rogers, R. D. *Dalton Trans.* **2004**, *15*, 2267–2271.

(36) (a) Mudring, A. V.; Babai, A.; Arenz, S.; Giernoth, R. *Angew. Chem., Int. Ed.* **2005**, *44*, 5485–5488. (b) Mezailles, N.; Ricard, L.; Gagosz, F. *Org. Lett.* **2005**, *7*, 4133. (c) Babai, A.; Mudring, A. V. *Z. Anorg. Allg. Chem.* **2008**, *634*, 938–940.

(37) Williams, D. B.; Stoll, M. E.; Scott, B. L.; Costa, D. A.; Oldham, W. J., Jr. *Chem. Commun.* **2005**, *11*, 1438–1440.

(38) Haas, A.; Klare, Ch.; Betz, P.; Bruckmann, J.; Krueger, C.; Tsay, Y.-H.; Aubke, F. *Inorg. Chem.* **1996**, *35*, 1918–1925.

(39) (a) Saalfrank, R. W.; Dresel, A.; Seitz, V.; Trummer, S.; Hampel, F.; Teichert, M.; Stalke, D.; Stadler, Ch.; Daub, J.; Schuenemann, V.; Trautwein, A. X. *Chem.—Eur. J.* **1997**, *12*, 2058–2062. (b) Rzepa, H. S.; Cass, M. E. *Inorg. Chem.* **2007**, *46*, 8024–8031. (c) Saalfrank, R. W.; Seitz, V.; Clauder, D. L.; Raymond, K. N.; Teichert, M.; Stalke, D. *Eur. J. Inorg. Chem.* **1998**, *9*, 1313–1317. (d) Saalfrank, R. W.; Seitz, V.; Heinemann, F. W.; Göbel, C.; Herbst-Irmer, R. *Dalton Trans.* **2001**, *5*, 599–603.

(40) Zahn, S.; Reckien, W.; Kirchner, B.; Staats, H.; Matthey, J.; Lützen, A. *Chem.—Eur. J.* **2009**, *15*, 2572–2580.